

See discussions, stats, and author profiles for this publication at: <https://www.researchgate.net/publication/224946059>

# A theoretical study of the vibrational spectrum of maleimide

ARTICLE *in* JOURNAL OF MOLECULAR STRUCTURE · MAY 2011

Impact Factor: 1.6 · DOI: 10.1016/j.molstruc.2010.10.042

---

CITATIONS

2

---

READS

138

3 AUTHORS, INCLUDING:



Eduardo Aguiar

Universidade Federal Rural de Pernambuco

4 PUBLICATIONS 13 CITATIONS

SEE PROFILE

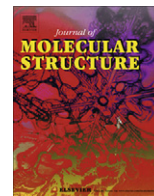


Joao Bosco Paraiso da Silva

Federal University of Pernambuco

55 PUBLICATIONS 347 CITATIONS

SEE PROFILE



# A theoretical study of the vibrational spectrum of maleimide

Eduardo C. Aguiar\*, João Bosco P. da Silva, Mozart N. Ramos

Departamento de Química Fundamental, Universidade Federal de Pernambuco (UFPE), 50670-901 Recife (PE), Brazil

## ARTICLE INFO

Article history:  
Available online 3 November 2010

Keywords:  
Maleimide  
Vibrational spectrum  
Theoretical calculations  
Infrared spectrum  
Anharmonicity

## ABSTRACT

B3LYP and MP2 theoretical calculations with 6-31++G(d,p) basis set have been performed to interpret the infrared spectrum of maleimide. The anharmonicity effect has been included to correct the calculated harmonic frequency values. As expected, this has allowed a better agreement with the experimental ones, especially B3LYP values. The more pronounced changes have been verified to the X–H (X = C or N) stretching modes.

The calculated IR intensities compare favorably well with their corresponding relative experimental values in vapor phase. The large discrepancy is found to the symmetric C–C stretching mode of the heterocyclic ring. It appears to be a strong band at  $897\text{ cm}^{-1}$ , in contrast to B3LYP and MP2 calculated values. The calculated intensities due to the out-of-plane and in-plane bending and stretching modes for the X–H oscillators (X = C or N) have been adequately interpreted in terms of hydrogen atomic charges and X–H charge-fluxes extracted from the modified charge–charge flux-overlap model (CCFOM) for infrared intensities.

© 2010 Elsevier B.V. All rights reserved.

## 1. Introduction

Maleimide (Fig. 1) and its *N*-derivatives have been employed in a variety of photochemical applications, which are based on their electron accepting properties [1]. Indeed, this represents the basis for modulating the fluorescence of compounds in which maleimide is incorporated. As a consequence, this modulation can be used to probe polymerization dynamics [2] or as a molecular sensor [3].

Nowadays, it is already well established that maleimide possesses a planar structure with  $C_{2v}$  symmetry [4]. It is interesting to point out that this planarity can be important to a possible biological activity of maleimide, once it has a molecular and electronic structure very similar to phthalimide. This latter is known to be a potent hypolipidemic agent. The loss of this planarity of the five-membered ring reduces, enormously, the hypolipidemic action in phthalimide [5].

In the last years, the chemistry of maleimide has been largely studied through combined studies involving vibrational spectroscopy and theoretical calculations [6–10]. In particular, Parker and collaborators [7] have combined infrared, Fourier Transform-Raman (FT-Raman), Inelastic Neutron Scattering (INS) spectroscopies and DFT calculations to provide the vibrational assignments of the spectra of maleimide and its *N*-derivatives. Barnes and collaborators [11] have also reported the infrared and Raman spectra for maleimide, *N*-deuterated maleimide and maleic anhydride in argon and nitrogen matrices and in the solid phase at 20 K. Furthermore, they have

investigated the interaction of maleimide with nitrogen, water and hydrogen chloride. This analysis has shown that water and hydrogen chloride form hydrogen-bonded complexes with a carbonyl group of the maleimide, whereas nitrogen interacts with the NH group. As a result, it is now well established that maleimide is expected to be monomeric only in the vapor phase and in dilute solutions [10], in contrast to what is found in maleic anhydride [12], which must be monomeric in all aggregation states. On the other hand, maleimide is expected to form dimer in concentrated solutions, melting and crystals [10], similarly to what happens with succinimide [13]. Recently, we have studied the effect of the H-bond formation in the molecular properties of maleimide in order to estimate the H-bond strength, frequency shifts and intensity enhancements after complexation [14].

This work aims to interpret the vibrational spectrum of maleimide using MP2 [15] and B3LYP [16] calculations with 6-31++G(d,p) basis set [17] through the Gaussian 03 program [18]. Here we have also analyzed the anharmonicity effect [19] on the molecular geometry and vibrational frequencies of maleimide, whereas its infrared intensities have been interpreted using the modified charge–charge flux-overlap model (CCFOM) [20,21].

## 2. Results and discussion

In Table 1 we give the optimized geometries with and without anharmonicity correction for maleimide using the MP2 and B3LYP levels of calculation with a 6-31++G(d,p) basis set. There we also include its available experimental values obtained from the

\* Corresponding author. Tel.: +55 81 21265007.

E-mail address: [castro.eduardo@gmail.com](mailto:castro.eduardo@gmail.com) (E.C. Aguiar).

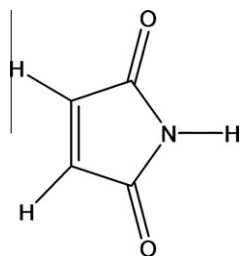


Fig. 1. Maleimide structure.

electron diffraction study in the gas phase [4]. In general, there is a good agreement between theoretical and experimental values. Except to N–H bond, the anharmonicity correction increases the chemical bond length for both the MP2 and B3LYP levels of calculation. This provokes a better agreement with the corresponding experimental values. The bond angles, in turn, practically are not affected by this correction.

### 2.1. Vibrational analysis

In Table 2 we show the vibrational assignments and frequencies, as well as infrared intensities of maleimide obtained from B3LYP and MP2 calculations using a 6-31++G(d,p) basis set. The anharmonicity effect on the vibrational frequencies is also shown in this Table, whereas experimental values in gas phase [10] and in argon matrix at 20 K [11] are also given for comparison. The 21 active IR fundamentals can be divided into  $9a_1 + 4b_1 + 8b_2$ . Initially, we can observe, from Table 2, that there is a good agreement between experimental and calculated spectra of maleimide, especially when the anharmonicity correction is introduced on the calculated values.

In order to better analyze these active IR modes of maleimide, we will divide its IR spectrum into three parts: (a) the region of the X–H stretching modes with X = C and N, (b) the region of the C=O stretching and (c) the region below the latter.

#### 2.1.1. (a) X–H stretching modes (X = C and N)

**2.1.1.1. (a.1) N–H stretching ( $a_1$ ).** The intense band at  $3482\text{ cm}^{-1}$  of the IR spectrum of maleimide in the vapor phase and  $3486\text{ cm}^{-1}$  in argon matrix is due to the N–H stretching, whereas the MP2 and B3LYP calculated values not including the anharmonicity correction are  $3710\text{ cm}^{-1}$  and  $3655\text{ cm}^{-1}$ , respectively. These values differ by ca.  $228\text{ cm}^{-1}$  and  $173\text{ cm}^{-1}$  to the experimental one. After correction, these differences fall to ca.  $57\text{ cm}^{-1}$  for MP2 and  $7\text{ cm}^{-1}$  for B3LYP. With respect to IR intensity, B3LYP and MP2 val-

ues, for this mode, confirm a strong intensity of  $91.5\text{ km mol}^{-1}$  and  $104.5\text{ km mol}^{-1}$ , respectively. This intensity can be adequately interpreted by Eq. (1) [22] shown below:

$$A^{\text{NH, str.}} = K \left( q_{\text{H}}^0 + \left( \frac{\partial q_{\text{H}}}{\partial R_{\text{N-H}}} \right) \cdot R_{\text{N-H}}^0 \right)^2 \quad (1)$$

where  $K = 975$  for intensity values in  $\text{km mol}^{-1}$ ,  $R_{\text{N-H}}^0$  stands for the equilibrium N–H bond length and  $q_{\text{H}}^0$  represents the hydrogen equilibrium charge, which is obtained from the Mulliken net charge corrected by the inclusion of overlap term from the CCFO model [20,21]. This means that the hydrogen charge is given by the  $p_{\text{H}}^{\text{xx}}$  element of the atomic polar tensor [23] of the hydrogen atom, where the 'x' axes is perpendicular to the molecular plane. The derivative  $\partial q_{\text{H}} / \partial R_{\text{N-H}}$  is the rate of variation of this charge with the stretching of the N–H bond. Previous works [22,24] have shown that this latter is small and negative for acid hydrogen atoms, i.e.,  $\equiv\text{C-H}$ ,  $=\text{N-H}$  and  $-\text{O-H}$ . Their values are situated between  $-0.01\text{ e \AA}^{-1}$  and  $-0.03\text{ e \AA}^{-1}$ . For the N–H oscillator, it is  $-0.02\text{ e \AA}^{-1}$  using B3LYP and MP2 calculations with large basis sets, including polarization and diffuse functions [14]. Here B3LYP and MP2 values for the  $p_{\text{H}}^{\text{xx}}$  element of the hydrogen atom in N–H are 0.328 e and 0.342 e, whereas their corresponding values for the  $R_{\text{N-H}}^0$  equilibrium distance are  $1.011\text{ \AA}$  and  $1.010\text{ \AA}$ , respectively. Using these values in Eq. (1), B3LYP and MP2 predicted intensities for the N–H stretching are  $92.4\text{ km mol}^{-1}$  and  $101.0\text{ km mol}^{-1}$ , respectively, which are in excellent agreement with the calculated ones.

**2.1.1.2. (a.2) C–H stretchings.** The symmetric ( $a_1$ ) and asymmetric ( $b_2$ ) C–H stretching modes fall at  $3104\text{ cm}^{-1}$  and  $3170\text{ cm}^{-1}$ , respectively, of the IR spectrum of maleimide in  $\text{CCl}_4/\text{CS}_2$  solution [10]. The symmetric mode in the vapor phase falls at  $3090\text{ cm}^{-1}$ , which is in very good agreement with the one in solution. It is interesting to point out that our B3LYP and MP2 calculations without anharmonicity correction indicate that the C–H symmetric stretching frequency value is greater than the asymmetric one, in contrast to what was found in Ref. [10]. For instance, B3LYP values for the symmetric and asymmetric C–H stretching frequencies are  $3270\text{ cm}^{-1}$  and  $3250\text{ cm}^{-1}$ , respectively. After anharmonicity correction, B3LYP values indicate to order verified in Ref. [10]. Its C–H symmetric stretching frequency including anharmonicity is  $3069\text{ cm}^{-1}$  whereas the corresponding C–H asymmetric frequency is  $3111\text{ cm}^{-1}$  in agreement with the experimental one. As expected, we can notice from Table 2 that the anharmonicity effect is much pronounced on these C–H stretching modes.

These symmetric and asymmetric C–H stretching intensities can also be adequately interpreted by using Eq. (1). We have seen that acid hydrogen atoms possess  $q_{\text{H}}^0$  large and positive whereas  $\partial q_{\text{H}} / \partial R_{\text{N-H}}$  is small and negative, and consequently, their X–H stretching intensities are mainly determined by hydrogen atomic charge. In C–H ethylenic hydrogen atoms, the situation is altered due to the increase of the charge-flux term. This latter becomes large and negative, and consequently, the charge and charge-flux terms are practically cancelled, i.e.,  $q_{\text{H}}^0 \cong -(\partial q_{\text{H}} / \partial R_{\text{C-H}})$ . As a result, their intensities are generally weak or very weak, as can be seen in Table 2. Another example, the sum of the symmetric and asymmetric C–H stretching intensities in  $\text{cis-C}_2\text{H}_2\text{F}_2$  is only  $3.5 \pm 3.5\text{ km mol}^{-1}$  [25].

The  $p_{\text{H}}^{\text{xx}}$  element representing the hydrogen atomic charge of the hydrogen atom in the ethylenic moiety in maleimide is 0.155 e for B3LYP and 0.163 e for MP2. The  $\partial q_{\text{H}} / \partial R_{\text{C-H}}$  charge-flux term can be obtained from the expression derived in Ref. [22], as shown to follow:

$$\frac{\partial q_{\text{H}}}{\partial R_{\text{C-H}}} = - \frac{[p_{\text{H}}^{\text{zy}} - (p_{\text{H}}^{\text{zz}} - p_{\text{H}}^{\text{xx}}) \cdot \text{tg}(\beta)]}{R_{\text{C-H}}^0 \cdot \text{tg}(\beta)} \quad (2)$$

Table 1

MP2/6-31++G(d,p) and B3LYP/6-31++G(d,p) anharmonic and harmonic optimized geometries of maleimide. B3LYP values are shown in parenthesis. Experimental values are given for comparison from Ref. [4]. Bond angles and distances are given in Å and degrees, respectively.

Parameter	Harmonic	Anharmonic	Experimental
H–C	1.079 (1.082)	1.081 (1.085)	1.091 <sup>a</sup>
H–N	1.010 (1.011)	0.999 (1.004)	1.020 <sup>a</sup>
C=C	1.346 (1.339)	1.349 (1.343)	$1.344 \pm 0.004$
C–C	1.498 (1.504)	1.504 (1.509)	$1.508 \pm 0.003$
C–N	1.396 (1.397)	1.403 (1.403)	$1.409 \pm 0.003$
C=O	1.224 (1.214)	1.224 (1.215)	$1.206 \pm 0.002$
C–N–C	111.7 (111.6)	111.4 (111.6)	$112.0 \pm 0.2$
N–C–C	105.4 (105.4)	105.5 (105.4)	$106.8 \pm 0.2$
N–C=O	126.3 (126.3)	126.2 (126.3)	$123.9 \pm 0.3$
H–C–C(O)	122.1 (121.8)	122.1 (121.8)	–

<sup>a</sup> Assumed parameters as in Ref. [4].

**Table 2**

MP2/6-31++G(d,p) and B3LYP/6-31++G(d,p) anharmonic and harmonic vibrational frequencies and IR intensities of maleimide. B3LYP values are given in parenthesis whereas experimental values from Ref. [10] are given in brackets and from Ref. [11] in curly brackets.

<i>i</i>	Mode	Assignments <sup>d</sup>	$\nu_i^{\text{harmonic}}$ (cm <sup>-1</sup> )	$\nu_i^{\text{anharmonic}}$ (cm <sup>-1</sup> )	IR intensities <sup>e</sup> (km mol <sup>-1</sup> )
1	b <sub>1</sub>	O=C–N–C=O bend.	92 (139)	208 (153)	0.0 (1.9)
2	a <sub>1</sub>	C=O bend.	389 (390) [400] <sup>a</sup> [410]	386 (390)	18.5 (19.6) [m] {m}
3	b <sub>1</sub>	N–H bend.	455 (513) [415] <sup>b</sup> [505]	579 (540)	108.3 (105.3) [s] {s}
4	b <sub>2</sub>	C=O bend.	536 (536) [552] <sup>c</sup> [536]	532 (534)	5.9 (2.9) [w] {w}
5	b <sub>1</sub>	C=O bend.	611 (632) [620] [624]	614 (622)	22.9 (10.9) [m] {w}
6	a <sub>1</sub>	Ring str.	638 (639) [637] [633]	628 (631)	2.2 (3.0) [vw] {vw}
7	b <sub>2</sub>	Ring bend.	679 (673) [668] [670]	669 (666)	25.7 (25.6) [s] {m}
8	b <sub>1</sub>	C–H bend.	783 (838) [831] [829]	840 (834)	72.4 (75.3) [s] {s}
9	a <sub>1</sub>	C–C str.	924 (907) [897] [895]	912 (896)	0.7 (1.4) [s] {w}
10	b <sub>2</sub>	Ring bend.	938 (921) [906] [905]	915 (902)	44.8 (35.8) [s] {s}
11	a <sub>1</sub>	C–H bend.	1101 (1084) [1057] <sup>a</sup> [1119]	1083 (1071)	9.3 (9.3) [w] {m}
12	b <sub>2</sub>	C–N–C str.	1174 (1141) [1130] [1132]	1140 (1108)	80.1 (46.3) [s] {s}
13	b <sub>2</sub>	C–H bend.	1351 (1321) [1285] [1285]	1324 (1306)	30.8 (5.4) [w] {m}
14	a <sub>1</sub>	C–N–C str.	1373 (1347) [1335] [1330]	1339 (1317)	140.0 (145.5) [s] {s}
15	b <sub>2</sub>	N–H bend.	1367 (1354) [1322] [1346]	1336 (1329)	13.0 (20.3) [m] {s}
16	a <sub>1</sub>	C=C str.	1632 (1644) [1580] [1574]	1609 (1559)	1.9 (1.1) [w] {vw}
17	b <sub>2</sub>	C=O str.	1794 (1803) [1756] [1744]	1752 (1768)	683.8 (847.0) [vs] {vs}
18	a <sub>1</sub>	C=O str.	1818 (1842) [1770] <sup>a</sup> [1770]	1774 (1828)	16.2 (27.5) [m] {s}
19	b <sub>2</sub>	C–H str.	3316 (3250) [3170] <sup>a</sup> {–}	3184 (3111)	0.2 (0.0) [vw] {–}
20	a <sub>1</sub>	C–H str.	3336 (3270) [3090] {–}	3236 (3069)	0.1 (0.0) [vw] {–}
21	a <sub>1</sub>	N–H str.	3710 (3655) [3482] [3486]	3539 (3489)	104.7 (91.5) [s] {s}

<sup>a</sup> This value is taken from the IR spectrum of maleimide of the CCl<sub>4</sub>/CS<sub>2</sub> solution in Ref. [10].

<sup>b</sup> This value is attributed to  $\nu_2$  in Ref. [10] and not to  $\nu_3$  as proposed here (see text).

<sup>c</sup> This value is taken from the IR spectrum of maleimide in the solid state;

<sup>d</sup> i.p. = in-phase and o.p. = out of phase.

<sup>e</sup> vs = very strong, s = strong, m = medium, w = weak and vw = very weak.

where  $p_{\text{H}}^{\text{zy}}$  is the  $\partial p_z / \partial y_{\text{H}}$  element of the atomic polar tensor of the hydrogen atom,  $\beta$  is the C=C–C angle and  $R_{\text{C–H}}^0$  is the C–H equilibrium distance. From this equation, we have obtained the following fluxes:  $-0.129 \text{ e } \text{\AA}^{-1}$  for B3LYP and  $-0.128 \text{ e } \text{\AA}^{-1}$  for MP2. Therefore, it becomes clear why the C–H stretching intensities in maleimide are weak or very weak. For instance, the term  $q_{\text{H}}^0 + (\partial q_{\text{H}} / \partial R_{\text{C–H}}) \cdot R_{\text{C–H}}^0$  is 0.015 for B3LYP and consequently, its predicted intensity for the C–H stretching mode is only  $0.2 \text{ km mol}^{-1}$ . Analogously, the corresponding predicted intensity for the MP2 calculations is  $0.6 \text{ km mol}^{-1}$ .

### 2.1.2. (b) C=O stretching modes

The IR spectrum of maleimide is mainly dominated by asymmetric C=O stretching mode (b<sub>2</sub>) at  $1756 \text{ cm}^{-1}$  in vapor phase,  $1738 \text{ cm}^{-1}$  in CCl<sub>4</sub>/CS<sub>2</sub> solution [10] and  $1744 \text{ cm}^{-1}$  in argon matrix [11]. In all conditions, this band is observed to be very strong, what is also confirmed by our theoretical calculations. Its B3LYP and MP2 values are  $847.0 \text{ km mol}^{-1}$  and  $683.8 \text{ km mol}^{-1}$ , respectively, whereas their corresponding frequency values including anharmonicity correction are  $1752 \text{ cm}^{-1}$  and  $1768 \text{ cm}^{-1}$ . These latter are in excellent agreement with its experimental value in vapor phase.

The symmetric (a<sub>1</sub>) C=O stretching intensity appears to be medium at  $1770 \text{ cm}^{-1}$  in both CCl<sub>4</sub>/CS<sub>2</sub> solution and argon matrix. This is also confirmed by our theoretical calculations, especially that B3LYP, i.e.,  $27.5 \text{ km mol}^{-1}$ .

From Table 2, we can note that both experimental and theoretical results show that the symmetric C=O stretching frequency is greater than the asymmetric one. According to Woldebaek et al. [10] this is mainly due to resonance stabilization involving the O=C–N–C=O moiety.

### 2.1.3. (c) Region below the C=O stretching

In this region there are nineteen active IR bands of maleimide, which are analyzed to follow:

**2.1.3.1. (c.1) C=C stretching mode (a<sub>1</sub>).** This mode seems to be weak at  $1580 \text{ cm}^{-1}$  in vapor phase,  $1583 \text{ cm}^{-1}$  in CCl<sub>4</sub>/CS<sub>2</sub> solution [10] and very weak at  $1574 \text{ cm}^{-1}$  in argon matrix [11]. This is also

confirmed by B3LYP and MP2 calculations, i.e.,  $1.1 \text{ km mol}^{-1}$  and  $1.9 \text{ km mol}^{-1}$ , respectively. Since maleimide possesses a C<sub>2v</sub> molecular symmetry, the dipole moment derivative associated with the C=C stretching intensity is located perpendicularly to C=C bond, similarly to what is also observed in *cis*-C<sub>2</sub>H<sub>2</sub>X<sub>2</sub> (X = F or Cl) [24].

**2.1.3.2. (c.2) Out-of-plane and in-plane N–H bending modes.** The out-of-plane N–H bending mode (b<sub>1</sub>) appears to be strong at  $513 \text{ cm}^{-1}$  for B3LYP and  $455 \text{ cm}^{-1}$  for MP2. As can be seen in Table 2, the anharmonicity effect is pronounced on this mode. After correction, these calculated values are  $579 \text{ cm}^{-1}$  for MP2 and  $540 \text{ cm}^{-1}$  for B3LYP. Their IR intensities are  $105.3 \text{ km mol}^{-1}$  and  $108.3 \text{ km mol}^{-1}$ , respectively. This value is essentially due to the equilibrium atomic charge of the hydrogen atom. Once the molecule is planar there are not charge-fluxes contributing to its intensity [26,27]. Thus, its IR intensity can be adequately represented by [22,24]:

$$A_{\text{N–H Bend}}^{\text{out-of-plane}} = K \cdot (q_{\text{H}}^0)^2 \quad (3)$$

We have already seen that the B3LYP and MP2 hydrogen atomic charges in N–H are 0.328 e and 0.341 e, respectively. Consequently, the out-of-plane N–H bending intensity is  $104.9 \text{ km mol}^{-1}$  for B3LYP and  $113.4 \text{ km mol}^{-1}$  for MP2, which are in very good agreement with the calculated ones. In fact, this band must have a strong intensity once it is determined by the atomic charge of acid hydrogen. It is already well established that this latter is large and positive, as our results have shown here. This result shows a better agreement with that obtained through argon matrix [11] when compared with that in CCl<sub>4</sub>/CS<sub>2</sub> solution [10].

The IR band relative to the in-plane N–H bending mode (b<sub>2</sub>) appears to be at  $1346 \text{ cm}^{-1}$  in argon matrix [11] and  $1340 \text{ cm}^{-1}$  in vapor phase [10]. These values are in good agreement with those obtained from B3LYP and MP2 calculations including anharmonicity correction, i.e.,  $1329 \text{ cm}^{-1}$  and  $1336 \text{ cm}^{-1}$ , respectively, whereas their corresponding IR intensities are  $20.3 \text{ km mol}^{-1}$  and  $13.0 \text{ km mol}^{-1}$ . It is still interesting to verify that this IR intensity is relatively decreased with respect to that of out-of-plane. This

is mainly due to the presence of the angular charge-flux term ( $\partial q_H / \partial \theta_{HCN}$ ), which is negative. This turns its IR intensity lower than that out-of-plane. This latter, as we have seen, only depends on the positive atomic charge of the hydrogen atom.

**2.1.3.3. (c.3) Out-of-plane and in-plane ring bending modes.** In general, there is a good agreement between experimental and calculated values for these ring bending modes, as can be seen in Table 2. The out-of-plane band at  $620\text{ cm}^{-1}$  in vapor phase appears to have a medium intensity, which is also confirmed by theoretical calculations. These latter are  $10.9\text{ km mol}^{-1}$  for B3LYP and  $22.9\text{ km mol}^{-1}$  for MP2, whereas its corresponding frequency values including anharmonicity correction are in very good agreement with the experimental one, i.e.,  $614\text{ cm}^{-1}$  and  $622\text{ cm}^{-1}$ , respectively.

The in-plane ring bending band ( $b_2$ ) at  $668\text{ cm}^{-1}$  in vapor phase and  $670\text{ cm}^{-1}$  in argon matrix also shows an excellent agreement with the B3LYP and MP2 calculated values including anharmonicity correction, i.e.,  $666\text{ cm}^{-1}$  and  $669\text{ cm}^{-1}$ , respectively. On the other hand, its IR observed intensity appears to be strong in vapor phase, but the theoretical results indicate a medium intensity, i.e.,  $25.6\text{ km mol}^{-1}$  for B3LYP and  $25.7\text{ km mol}^{-1}$  for MP2, which are in agreement with that obtained in argon matrix.

**2.1.3.4. (c.4) C–N–C and C–C stretching modes.** The IR bands due to the symmetric ( $a_1$ ) and asymmetric ( $b_2$ ) C–N–C stretching modes at  $1335\text{ cm}^{-1}$  and  $1130\text{ cm}^{-1}$ , respectively, show a very good agreement with their calculated values including anharmonicity correction. For instance, their MP2 values for the symmetric and asymmetric modes are  $1339\text{ cm}^{-1}$  and  $1140\text{ cm}^{-1}$ , respectively. These modes appear to have strong intensities in vapor phase. This is also confirmed by our theoretical calculations, especially that MP2, i.e.,  $140.0\text{ km mol}^{-1}$  and  $80.1\text{ km mol}^{-1}$ , respectively.

The in-phase C–C symmetric stretching ( $a_1$ ) mode appears to be strong at  $897\text{ cm}^{-1}$  in vapor phase in contrast to what is observed in argon matrix. This later shows a weak band in  $895\text{ cm}^{-1}$  which is agreement with the calculated ones, i.e.  $0.7\text{ km mol}^{-1}$  for MP2 and  $1.4\text{ km mol}^{-1}$  for B3LYP. The out-of-phase C–C stretching mode ( $b_2$ ) at  $906\text{ cm}^{-1}$  in vapor phase and  $905\text{ cm}^{-1}$  in argon matrix shows a very good agreement with its corresponding MP2 and B3LYP values including anharmonicity correction, i.e.,  $915\text{ cm}^{-1}$  and  $902\text{ cm}^{-1}$ , respectively. This mode appears to have a strong intensity, which is also confirmed by B3LYP and MP2 results.

**2.1.3.5. (c.5) Out-of-plane and in-plane C–H bending modes.** The in-plane C–H bending ( $b_2$ ) mode at  $1285\text{ cm}^{-1}$  in vapor phase only shows a reasonable agreement with its MP2 and B3LYP calculated values including or not anharmonicity correction. For instance, its MP2 not corrected value is  $1351\text{ cm}^{-1}$  and anharmonicity correction after is  $1324\text{ cm}^{-1}$ . The difference of this latter with respect to the experimental value is still reasonably large, i.e.,  $39\text{ cm}^{-1}$ . Its IR intensity is observed to be weak in vapor phase, which is also confirmed by B3LYP theoretical calculations, i.e.,  $5.4\text{ km mol}^{-1}$ . Nevertheless, its MP2 value is  $30.8\text{ km mol}^{-1}$ , which agrees with the medium intensity in argon matrix.

On the other hand, the observed frequency for the out-of-plane C–H bending ( $b_1$ ) mode at  $831\text{ cm}^{-1}$  in vapor phase and  $829\text{ cm}^{-1}$  in argon matrix shows a very good agreement with its MP2 and B3LYP calculated values including anharmonicity correction, i.e.,  $840\text{ cm}^{-1}$  and  $834\text{ cm}^{-1}$ , respectively, as can be seen in Table 2. Both MP2 and B3LYP calculations predict a strong intensity for this mode, confirming experimental results, i.e.,  $72.4\text{ km mol}^{-1}$  and  $75.3\text{ km mol}^{-1}$ , respectively. In contrast to the out-of-plane N–H bending intensity, the out-of-plane C–H mode is not completely located in the hydrogen atoms of the ethylenic moiety in maleimide. Thus, it is not possible directly to use Eq. (3). In order to

better estimate its value, it becomes necessary to introduce the weight of the normal coordinate ( $\lambda$ ) associated with the two hydrogen atoms in  $-\text{CH}=\text{CH}-$ , as well as their atomic charges. As a consequence, Eq. (3) becomes (Eq. (4)):

$$A_{\text{C-H Bend}}^{\text{out-of-plane}} = K \cdot \lambda \cdot (2 \cdot q_H^0)^2 \quad (4)$$

where  $\lambda$  is 0.67 for B3LYP and 0.68 for MP2. Considering their corresponding atomic charges of 0.155 e and 0.163 e obtained from the  $p_H^{\text{xx}}$  element of the atomic polar tensor of the hydrogen atom of the ethylenic moiety in maleimide, B3LYP and MP2 predicted intensities are  $62.8\text{ km mol}^{-1}$  and  $70.5\text{ km mol}^{-1}$ , respectively, which are in good agreement with the experimental ones.

### 3. Conclusions

Our B3LYP/6-31++G(d,p) and MP2/6-31++G(d,p) calculations have been successful in interpreting the IR spectrum of maleimide. In general, there is a very good agreement between experimental and calculated values, especially in terms of vibrational frequencies including anharmonicity correction. Our calculations have been particularly useful to help in the vibrational assignments of the IR bands with weak or very weak intensities. The out-of-plane and in-plane bending and stretching modes for the X–H oscillators with X = C or N have been adequately interpreted in terms of the modified charge–charge flux–overlap model for infrared intensities.

### Acknowledgements

The authors gratefully acknowledge financial support from the Brazilian funding agencies: CNPq, CAPES and FINEP.

### References

- [1] J. von Soutag, W.J. Knolle, Photochem. Photobiol. A: Chem. 136 (2000) 133.
- [2] J.M. Warman, R.D. Abellon, H.J. Verhey, J.W. Verhoeven, J.W. Hofstraal, J. Phys. Chem. B 101 (1977) 4913.
- [3] B.K. Kaletas, R.M. Williams, B. König, L. De Cole, Chem. Commun. (Cambridge) (2002) 776.
- [4] L. Harsányi, E. Vajda, I. Hargittai, J. Mol. Struct. 129 (1985) 315.
- [5] (a) A.R.K. Murthy, O.T. Wong, D.J. Reynolds, I.H. Hall, Pharm. Res. 4 (1987) 2; (b) M.N. Ramos, B.B. Neto, J. Comput. Chem. 11 (1990) 569.
- [6] C. Corsaro, S.F. Parker, Physics B 350 (2004) 591.
- [7] S.F. Parker, Spectrochim. Acta A 51 (1995) 2067.
- [8] S.F. Parker, Spectrochim. Acta A 63 (2006) 544.
- [9] D.H.A. Steege, W.J.J. Buma, Chem. Phys. 118 (2003) 10944.
- [10] T. Woldbaek, P. Klaboe, C.J. Nielsen, J. Mol. Struct. 27 (1975) 283.
- [11] A.J. Barnes, L. Le Gall, C. Madec, J. Lauransan, J. Mol. Struct. 38 (1977) 109.
- [12] A. Rogstad, P. Klaboe, H. Baranska, E. Bjarnov, D.H. Christensen, F. Nicolaisen, O.F. Nielsen, N.B. Cyvin, S.J. Cyvin, J. Mol. Struct. 20 (1974) 403.
- [13] R. Mason, Acta Crystallogr. 14 (1961) 720.
- [14] E.C. Aguiar, J.B.P. da Silva, M.N. Ramos, Spectrochim. Acta A 71 (2008) 5.
- [15] C. Möller, M.S. Plesset, Phys. Rev. 46 (1934) 618.
- [16] A.D.J. Becke, J. Chem. Phys. 98 (1993) 5648.
- [17] (a) W.J. Hehre, R. Ditchfield, J.A. Pople, J. Chem. Phys. 56 (1972) 2257; (b) R. Krishnan, J.S. Binkley, R. Seeger, J.A. Pople, J. Chem. Phys. 72 (1980) 650.
- [18] M.J. Frisch, G.W. Trucks, M. Head-Gordon, P.M.W. Gill, M.W. Wong, J.B. Foresman, B.G. Johnson, H.B. Schlegel, M.A. Robb, E.S. Replogle, R. Gomperts, J.L. Andres, K. Raghavachari, J.S. Binkley, C. Gonzalez, R.L. Martin, D.J. Fox, D.J. Defrees, J. Baker, J.J.P. Stewart, J.A. Pople, Gaussian 98W (revision A11.2), Gaussian, Inc., Pittsburgh, PA, 2001.
- [19] V. Barone, J. Chem. Phys. 122 (2005) 014108.
- [20] W.T. King, G.B. Mast, J. Phys. Chem. 80 (1976) 2521.
- [21] M. Gussoni, M.N. Ramos, C. Castiglioni, G. Zerbi, Chem. Phys. Lett. 142 (1987) 515.
- [22] (a) M. Gussoni, J. Mol. Struct. 141 (1986) 63; (b) M. Gussoni, C. Castiglioni, M.N. Ramos, M. Rui, G. Zerbi, J. Mol. Struct. 224 (1990) 445.
- [23] W.B. Person, J.H. Newton, J. Chem. Phys. 61 (1974) 1040.
- [24] M.N. Ramos, R. Fausto, J.J.C. Teixeira-Dias, C. Castiglioni, M. Gussoni, G. Zerbi, J. Mol. Struct. 248 (1991) 281.
- [25] R.O. Kagel, D.L. Powell, J. Overend, M.N. Ramos, A.B.M.S. Bassi, R.E. Bruns, J. Chem. Phys. 78 (1983) 7029.
- [26] M.N. Ramos, M. Gussoni, C. Castiglioni, G. Zerbi, Chem. Phys. Lett. 151 (1988) 397.
- [27] U. Dinur, Chem. Phys. Lett. 166 (1990) 211.